HHS Public Access

Author manuscript

Int J Radiat Oncol Biol Phys. Author manuscript; available in PMC 2015 March 25.

Published in final edited form as:

Int J Radiat Oncol Biol Phys. 2012 July 1; 83(3): 972–979. doi:10.1016/j.ijrobp.2011.08.011.

Characterizing Tumor Heterogeneity With Functional Imaging and Quantifying High-Risk Tumor Volume for Early Prediction of Treatment Outcome: Cervical Cancer as a Model

Nina A. Mayr, M.D.[*], **Zhibin Huang, Ph.D.**[†], **Jian Z. Wang, Ph.D.**[*], **Simon S. Lo, M.D.**[‡], **Joline M. Fan, B.S.**[§], **John C. Grecula, M.D.**[*], **Steffen Sammet, M.D., Ph.D.**[¶,‖], **Christina L. Sammet, Ph.D.**[¶], **Guang Jia, Ph.D.**[‖], **Jun Zhang, Ph.D.**[‖], **Michael V. Knopp, M.D., Ph.D.**[‖], and **William T.C. Yuh, M.D., M.S.E.E.**[‖]

[*]Department of Radiation Oncology, Ohio State University, Columbus, OH

[†]Department of Radiation Oncology and Department of Physics, East Carolina University, Greenville, NC

[‡]Department of Radiation Oncology, Case Western Reserve University, Cleveland, OH

[§]Department of Molecular Biology, Stanford University, Stanford, CA

[¶]Department of Radiology, University of Chicago, Chicago, IL

[‖]Department of Radiology, Ohio State University, Columbus, OH

Abstract

Purpose—Treatment response in cancer has been monitored by measuring anatomic tumor volume (ATV) at various times without considering the inherent functional tumor heterogeneity known to critically influence ultimate treatment outcome: primary tumor control and survival. This study applied dynamic contrast-enhanced (DCE) functional MRI to characterize tumors' heterogeneous subregions with low DCE values, at risk for treatment failure, and to quantify the functional risk volume (FRV) for personalized early prediction of treatment outcome.

Methods and Materials—DCE-MRI was performed in 102 stage IB_2–IVA cervical cancer patients to assess tumor perfusion heterogeneity before and during radiation/chemotherapy. FRV represents the total volume of tumor voxels with critically low DCE signal intensity (<2.1 compared with precontrast image, determined by previous receiver operator characteristic analysis). FRVs were correlated with treatment outcome (follow-up: 0.2–9.4, mean 6.8 years) and compared with ATVs (Mann-Whitney, Kaplan-Meier, and multivariate analyses).

Results—Before and during therapy at 2–2.5 and 4–5 weeks of RT, FRVs >20, >13, and >5 cm^3, respectively, significantly predicted unfavorable 6-year primary tumor control ($p = 0.003$, 7.3×10^{-8}, 2.0×10^{-8}) and disease-specific survival ($p = 1.9 \times 10^{-4}$, 2.1×10^{-6}, 2.5×10^{-7},

Reprint requests to: Nina A. Mayr, M.D., Department of Radiation Oncology, Ohio State University, Arthur G. James Cancer Hospital, 300 W 10th Avenue, Columbus, OH 43210. Tel: (614) 293-3250; Fax: (614) 293-4044; Nina.Mayr@osumc.edu.

Presented at American Society for Therapeutic Radiology and Oncology Annual Meeting, San Diego, CA, October 31, 2010.

Conflict of interest: none.

respectively). The FRVs were superior to the ATVs as early predictors of outcome, and the differentiating power of FRVs increased during treatment.

Discussion—Our preliminary results suggest that functional tumor heterogeneity can be characterized by DCE-MRI to quantify FRV for predicting ultimate long-term treatment outcome. FRV is a novel functional imaging heterogeneity parameter, superior to ATV, and can be clinically translated for personalized early outcome prediction before or as early as 2–5 weeks into treatment.

Keywords

Tumor heterogeneity; Magnetic resonance imaging (MRI); Dynamic contrast enhanced (DCE) MRI; Cervical cancer; Anatomic tumor volume; Functional tumor imaging

Introduction

A daily dilemma in managing cancer patients is the heterogeneous therapy responsiveness among different patients with the same tumor stage (1, 2) and even among different subregions within the same tumor (3). Contrary to routinely available “culture and sensitivity tests” to assess the effectiveness of a specific antibiotic agent for a specific infection in individual patients, “therapeutic sensitivity” testing to assess the effectiveness of a specific cancer therapy before or early during treatment is generally lacking.

Such tumor heterogeneity and the inability to reliably predict the long-term treatment outcome for individual patients presents a major challenge in the treatment of advanced cervical cancer (1, 2). Despite best standard-of-care concurrent radiation/chemotherapy, cure rates have not improved over the past decade, and treatment fails in approximately one third of patients (4, 5). Treatment regimens for Stages IIB–IVA are fairly uniform despite profound variability in tumor control and survival (6, 7). Although there is suggestion that more intense therapies may improve outcome (8), it remains a challenge to triage the use of intensified therapies for standard-of-care and clinical trial regimens (1, 2).

On the basis of the current established International Federation of Gynecology and Obstetrics (FIGO) staging and the anatomic tumor volume (ATV)-based response criteria (9, 10), treatment failure is frequently not detected until many months after the completion of primary therapy. At such delayed time, salvage treatment options have limited impact on the ultimate long-term treatment outcome: primary tumor control and survival (11). Therefore, early prediction of failure from an ongoing treatment is the key to enable a therapeutic window to target intensified therapy to those patients with a higher risk of failure.

Heterogeneity of tumor microenvironment has been reported with respect to regional vascular density and hypoxia, proliferation, energy metabolism, and gene expression of tumors (12–15). Although the concept of tumor heterogeneity has not been incorporated into the current clinical oncology practice nor the evidence-based cancer treatment paradigm, there is ample evidence that heterogeneous functional/biological properties of tumors profoundly influence treatment outcome (3, 12, 16, 17). With the notion of variable therapy responsiveness at different subregions within the same tumor (3, 16, 17), treatment failure is

more critically influenced by at-risk subregions of the tumor, which possess unfavorable functional/biological properties, including poor perfusion and hypoxia (18–20). However, tumor heterogeneity is challenging to characterize and quantify in the clinical setting. Tissue biopsies are invasive and provide only limited sampling points of the entire heterogeneous tumor volume (21, 22). A novel noninvasive means to characterize functional heterogeneity throughout the entire tumor mass and quantify all at-risk subregions with unfavorable functional/biological properties, *i.e.*, the tumor's functional risk volume (FRV), would provide additional information to enhance the accuracy for early outcome prediction of a specific treatment in individual patients.

Dynamic contrast-enhanced (DCE) MRI has been valuable in assessing the microvascular structure and functional environment of tumors (23–26). DCE-MRI–based tumor perfusion status reflects the effective delivery of chemotherapy agents (12, 17, 27, 28) and oxygen (29) to tumor cells, both closely related to therapy responsiveness, tumor control and survival (17–19, 28). In cervical cancer, the well-established relationship between tumor vascularity, hypoxia, and radiation therapy response (18, 19) provides a unique tumor-biological basis to apply DCE perfusion imaging in clinical patients and explore DCE functional parameters to enhance the capability for early outcome prediction (30, 31). Poor perfusion status, reflected by low mean DCE value, has been associated with poor treatment outcome in cervical cancer (24, 31–36).

With the improved spatial and temporal resolution, clinical DCE-MRI would provide a unique opportunity to evaluate the heterogeneous functional/biological microenvironment throughout the entire tumor volume. High-precision three-dimensional (3D) anatomic and functional MRI are now available in the clinical setting (33). However, despite the promising reported correlations of tumor perfusion and treatment outcome (33–35, 37), clinical DCE imaging has not been routinely applied to characterize functional heterogeneity in clinical cervical cancer patients.

We have developed a voxelwise approach of DCE imaging to characterize each tumor voxel's perfusion status and quantify variations in tumor perfusion throughout the heterogeneous tumor mass (36, 38). Such methodology can be readily translated into the clinical arena to assess DCE-MRI-based tumor heterogeneity and define at-risk tumor voxels with unfavorable DCE values. FRV can be derived from the summation of at-risk tumor voxels with low perfusion and hypoxia (29), which adversely affect radiation response and survival (17–20, 28, 39).

The purpose of this study was to (*1*) functionally characterize tumor heterogeneity and quantify the FRV, defined as the volume of critically low DCE voxels, within the heterogeneous tumor; (*2*) clinically validate the predictive power of FRV at different time points of treatment for ultimate treatment outcome by correlation with long-term tumor control and disease-specific survival; and (*3*) compare the independent power of FRV with that of ATV at different treatment time points for early prediction of outcome.

Methods and Materials

Patient population

DCE-MRI was performed in 102 Stage IB_2–IVA cervical cancer patients accrued between 1994 and 2003. Patient characteristics are detailed in Table 1. Pretreatment evaluations included routine workup following the (FIGO) staging guidelines. Tumor therapy consisted of standard combined external beam radiation therapy with 6- to 24-MeV photon beams, concurrent weekly cisplatin-based chemotherapy, and standard brachytherapy. The external beam radiation dose to the pelvis ranged from 39.6 to 55.0 Gy (mean, 47.8 Gy) and was given at 1.8 to 2.0 Gy per fraction. All but four patients had brachytherapy, with Point A doses ranging from 14 to 61 Gy (mean, 39.5 Gy). Those without brachytherapy had external beam radiation therapy to a dose of 66.6 Gy using field reductions.

MRI protocol

Three serial MRI studies were performed on an institutional review board–approved protocol at three defined time points: before radiation therapy, early during the treatment course at 2–2.5 weeks into treatment (corresponding to a dose of 20–25 Gy), and midway into treatment at 4–5 weeks (45–50 Gy). All MRI examinations were obtained from 1.5-T scanners. Precontrast imaging protocols included sagittal precontrast T2-weighted imaging (repetition time/effective echo time = 4000/104 msec, echo train length = 10, number of excitations = 2) for tumor delineation as described in detail earlier (32). For the initial phase of the study, DCE-MRI used T1-weighted fast spin-echo sequences (repetition time/effective echo time =150/18 msec, echo train length =4, number of excitations = 1) at 3-second intervals and a bolus injection of Gadolinium-based contrast agent (0.1 mmol/kg). More recently DCE-MRI acquisition consisted of a T1-weighted 3D gradient echo multislice sequence (echo time =5 ms, TR =12 ms, Flip = 25°, FOV = 25 × 40 cm^2, Matrix = 138 × 256, Partition = 12, number of excitations =1, Slab =8.0 cm, Z oversample =40%) (31, 38). The tumor voxel size ranged from 20 to 65 mm^3. The patients' therapy was not influenced or modified by any MRI findings.

Image analysis

The tumor region was delineated on the T2-weighted image by three reviewers (NAM, WTY, and JZW). The anatomical 3D tumor volume (ATV) at the three time points (before treatment [ATV_1], during early therapy at 2–2.5 weeks [ATV_2], and midtherapy at 4–5 weeks [ATV_3]) was derived by summation of all tumor voxels within the tumor region based on the tumor delineation from the T2-weighted images as described previously (Fig. 1a and 1e) (36). Using the first-pass DCE method (30), a time-signal intensity (SI) DCE curve was generated for each tumor voxel (Fig. 1c and 1g). Tumor voxel SI histograms (Fig. 1d and 1h), first developed in our laboratory, were derived for each individual tumor at all three time points to depict the distribution of the entire tumor voxel population (*y* axis) and their DCE values (plateau SI, *x* axis) as described in detail earlier (36). Tumor heterogeneity can be readily appreciated on the voxel SI histogram as a wide range distribution of SI values of the entire tumor voxel population.

Functional risk volume

Tumor voxels with relatively lower DCE values were identified on the voxel- histogram (Fig. 1d and 1h). The functional at-risk tumor voxels were classified as those voxels with an SI < 2.1 (Fig. 1d and 1h), based on prior receiver operating characteristic (ROC) analysis that discriminated favorable from unfavorable treatment outcome (31). FRV was then derived by summation of the total number of the at-risk voxels within the tumor volume at each imaging time point (FRV_1, FRV_2, and FRV_3) obtained at the pre-therapy, early-therapy, and mid-therapy time points, respectively.

Clinical follow-up and data collection

Patients were evaluated posttherapy in 3- to 12-month intervals until death or last contact. Median follow-up of surviving patients, calculated from therapy completion, was 6.8 years (range, 0.2–9.4 years). Primary (local) tumor control was defined as absence of histologically proven recurrence or progression of the primary tumor in the cervix, uterus, or pelvis. For disease-specific survival, death from cervical cancer or complications of cancer was scored as event, and death of intercurrent disease was censored.

Statistical analysis

FRVs at each treatment imaging time point (FRV_1, FRV_2, and FRV_3) were correlated with primary tumor control and disease-specific survival endpoints (Mann-Whitney test). The optimal volume cutpoint values of FRVs at each imaging time point to differentiate the disease-specific survival vs. death were determined by ROC analysis. These optimal cutpoint values for FRVs were then applied for FRV_1, FRV_2, and FRV_3, respectively, to correlate with primary tumor control and disease-specific survival (Kaplan-Meier analysis, log-rank test). The corresponding ATVs and FRVs at the same treatment time point were compared as independent predictors for the early prediction of long-term treatment outcome using multivariate analysis.

Results

FRVs and ATVs obtained at the different treatment time points are summarized in Table 2. Overall, the mean FRVs were smaller than the ATVs at the corresponding imaging time points. Both ATVs and FRVs showed a wide range within clinical tumor stages and steadily decreased during the treatment course (Table 3).

ROC analysis identified the optimal cut-point values of the FRV at each treatment time point, which significantly discriminated disease-specific survival vs. death of cancer (Table 4). The optimal cutpoint values for FRV_1, FRV_2, and FRV_3 were 20 cm^3 (area under the curve [AUC] = 0.705), 13 cm^3 (AUC = 0.799), and 5 cm^3 (AUC = 0.796), respectively.

FRV_1, FRV_2, and FRV_3 were significant early predictors of ultimate long-term treatment outcome, clinically validated by the outcome endpoints of primary tumor control and disease-specific survival rate (Tables 3 and 4, Fig. 2) with a mean posttherapy follow-up of 6.8 years. The predictive power of FRVs for treatment outcome also increased during the treatment course (Tables 3, and 4, Fig. 2). Pretreatment FRV_1 had the least predictive power

when compared with the intratreatment FRV_2 and FRV_3 based on the magnitude of differences in outcome. The differences discriminated by FRV in the predicted 6-year actuarial tumor control rate vs. primary tumor recurrence increased from 24.3% for FRV_1 to 42.5% for FRV_2 and 45.2% for FRV_3 (Table 3, Fig. 2a–2c). The differences in disease-specific survival rate vs. cancer death increased from 41.5% to 47% and 48.5%, respectively (Table 4, Fig. 2d–2f). Multivariate analysis showed that FRV_2 and FRV_3 were superior to the ATVs as independent predictors of tumor control and disease-specific survival (Table 5).

Discussion

Improvement of outcome by early prediction of treatment failure

Overall approximately one third of advanced cervical cancer patients fail standard first-line treatment (6, 40) despite extensive use of concurrent radiation and chemotherapy and high-end clinical imaging. Although heterogeneous treatment response throughout Stage IB_2–IVA cervical cancer is well known, the treatment regimen remains largely uniform (“one size fits all”) for patients across these tumor stages (6, 7). The lack of personalized treatment strategy for individual patients, known to have heterogeneous treatment outcome (1, 2), likely plays an important role in the lack of improvement in treatment outcomes over the past decade (4). To provide personalized treatment strategy, early prediction of treatment outcome for each individual patient is key. Thus it is paramount to identify this significant number of high-risk patients early during their treatment course to provide a window of opportunity for adaptive therapy. In addition, low-risk patients, predicted early to have favorable treatment outcome, may benefit from less-intense therapy regimens, thereby reducing treatment-related morbidity, mortality, and health care cost.

Integration of morphologic and functional imaging methods to characterize tumor heterogeneity and target at-risk tumor subvolume (FRV) for early outcome prediction

Prediction of treatment failure is particularly challenging to make before or early during the treatment course, when targeted adjustments in therapy are more available and generally more effective (6, 11). By applying the known underlying pathophysiologic principles of low perfusion, hypoxia, and therapy resistance (17–20, 28, 39), our results support our hypothesis that the low-DCE subvolumes (FRV) within the heterogeneous tumor volume contribute to unfavorable treatment outcome. The at-risk tumor voxels with poor perfusion, critically low enough to result in therapy failure, were classified as having a DCE SI value <2.1, which had been validated previously (31). In our current research, both high-resolution 3D anatomic and functional imaging methodologies were integrated to target more effectively the essential underlying biology, and to more precisely derive FRV throughout the entire tumor with precision at the tumor voxel level. Such integrated imaging approach overcomes the challenge of irregular tumor morphology from the World Health Organization and Response Evaluation Criteria in Solid Tumors methodologies (9, 10), as well as the limitations of mean DCE values, averaged over the entire tumor volume, which do not characterize tumor heterogeneity (31). Furthermore, our methodology eliminates the need for tedious imaging manipulation to identify and match each tumor voxel sequentially at different treatment time points. Rather, our approach was to analyze the overall critical mass of at-risk voxels within the entire tumor at different treatment time points for outcome

prediction. Although our methodology does not achieve precision at the microscopic/cellular level, it provides a noninvasive practical approach of functional heterogeneity assessment throughout the entire tumor region with a precision equivalent to single imaging voxel size currently available in the clinical setting.

Clinical validation and database

Advanced cervical cancer is an ideal model for ultra-early imaging and clinical validation of early outcome prediction, because it is not treated surgically, allowing sequential imaging before and during treatment. Because most treatment failures occur within 2 years, our patient cohort provided solid clinical endpoints for statistical analysis and clinical validation of the novel FRV concept and its predictive power. Although these results may be limited by the relatively small patient numbers and the relatively large number of imaging parameters, our study has the largest patient population with DCE MRI in cervical cancer with the longest follow-up reported to date.

FRV cutpoint values

ROC analysis defined the optimal cutpoint values of the FRV at different treatment time points (FRV_1 = 20 cm^3, FRV_2 = 13 cm^3, and FRV_3 = 5 cm^3) to differentiate patients with favorable vs. unfavorable treatment outcome (Tables 3 and 4, Fig. 2). Such integrated morphologic and functional imaging approach provides a robust methodology that can readily translate into the clinical setting to guide therapy strategy. Our results further suggest that treatment failure depends not only on how low the voxels' DCE value is (quality of low perfusion) but also on the critical mass of low-DCE subvolume within the tumor (quantity of low perfusion; Tables 3 and 4, Fig. 2). FRV contains both these metrics and translates this critical functional imaging information into clinically significant therapy resistance to radiation and chemotherapy and unfavorable treatment outcome. Low-DCE volumes (FRV) as small as 13 cm^3 in early therapy (20–25 Gy) and 5 cm^3 in midtherapy (40–50 Gy) within the heterogeneous tumor were shown to impart primary tumor recurrence and cancer death (Tables 3 and 4, Fig. 2).

FRVs during treatment

In addition to FRV, the efficacy for early prediction of outcome also depends on the ability to incorporate essential information of the "therapeutic sensitivity" of a tumor to an ongoing therapy regimen. Such essential therapy-specific sensitivity information can only be reflected by the imaging parameters that are obtained *during* the treatment course, rather than those before treatment. FRVs decreased during the ongoing course of fractionated radiation therapy (Table 2), likely because of cell kill, both within the FRVs, and, to a greater degree, in the non-FRV tumor regions. Cell kill within the initial poorly perfused/oxygenated FRVs likely improves during ongoing radiotherapy through improvement of perfusion and reoxygenation. Patients with smaller subsequent FRVs had better outcome.

Our results show that the predictive power improved as early as 2 weeks into treatment (FRV_2) compared with the pretherapy imaging (FRV_1; Tables 3 and 4). Although the FRV_3 at the fourth–fifth treatment week (40–50 Gy) suggests a slight trend of better outcome prediction (Tables 3 and 4, Fig. 2, Kaplan-Meier analysis), FRV_2 enables treatment outcome

prediction at a much earlier time point in the second treatment week, when only approximately one fourth of the total radiation dose and 2 of the 5–7 chemotherapy cycles have been given. At that time, there is greater latitude to implement very early adjustments of the cytotoxic therapy regimen. However, the comparative efficacy between FRV_2 and FRV_3 remains to be determined in future studies. In addition, the comparative or complementary value of other functional imaging modalities, *e.g.*, diffusion MRI or PET, remains to be determined.

Comparison of FRV and ATV

Our results support the notion that the FRVs during therapy are superior to the ATVs obtained at the corresponding time points for early prediction of treatment outcome (Table 5). The addition of functional/biological information significantly improves the ability to predict tumor control and survival compared with morphologic tumor volume alone. Among our patient group, FRV and ATV were highly variable (Table 2), indicating that heterogeneity was pervasive across the traditional morphological tumor volume, clinical FIGO stage categories and imaging time points. This observation indirectly supports the concept that current established clinical criteria, including FIGO stage, World Health Organization, and Response Evaluation Criteria In Solid Tumors (9, 10), have inherent limitations for early outcome prediction and may play a role for our inability to implement timely personalized treatment strategy and the lack of improvement in treatment outcome.

Conclusion

Our results suggest that tumor-heterogeneity-based DCE parameters provide essential information of tumor biological/functional properties that critically influence long-term treatment outcome. The ability to characterize DCE heterogeneity by a voxelwise approach, classify the at-risk tumor voxels, and quantify FRV significantly improves early prediction of treatment outcome over the traditional morphology-based ATV. Therefore, FRVs are potential novel heterogeneity parameters that can augment the current established clinical staging and ATV response criteria. If reconfirmed with future studies, FRVs at various treatment time points can serve as noninvasive early outcome predictors for clinical translation and may guide therapy adaptation as a personalized theranostic paradigm to further improve treatment outcome. This new FRV concept and our methodology may also be applicable to derive tumor heterogeneity parameters in other tumors to enhance cancer therapy and to improve clinical trials by focusing novel cancer therapy regimens at more targeted patient cohorts with higher risk of therapy failure.

Acknowledgments

Nina A. Mayr and William T. C. Yuh are supported by National Institute of Health Grant No. RO1 CA71906.

This work is dedicated to Jian Z. Wang, Ph.D., who critically contributed to this research. Dr. Wang tragically passed away in 2010.

References

1. Eifel PJ. Problems with the clinical staging of carcinoma of the cervix. Semin Radiat Oncol. 1994; 4:1–8. [PubMed: 10717083]

2. Eifel PJ, Morris M, Wharton JT, et al. The influence of tumor size and morphology on the outcome of patients with FIGO stage IB squamous cell carcinoma of the uterine cervix. Int J Radiat Oncol Biol Phys. 1994; 29:9–16. [PubMed: 8175451]
3. Lyng H, Vorren AO, Sundfor K, et al. Intra- and intertumor heterogeneity in blood perfusion of human cervical cancer before treatment and after radiotherapy. Int J Cancer. 2001; 96:182–190. [PubMed: 11410887]
4. International Agency for Research on Cancer, World Health Organization. Globocan 2008. Cervical cancer incidence and mortality worldwide in 2008. Summary. Available at: http://globocan.iarc.fr/factsheets/cancers/cervix.asp#MORTALITY
5. American Cancer Society. Global cancer facts and figures 2007. 2007. Available at: http://www.cancer.org/downloads/STT/Global_Cancer_Facts_and_Figures_2007_rev.pdf
6. Eifel PJ, Winter K, Morris M, et al. Pelvic irradiation with concurrent chemotherapy versus pelvic and para-aortic irradiation for high-risk cervical cancer: An update of radiation therapy oncology group trial (RTOG) 90-01. J Clin Oncol. 2004; 22:872–880. [PubMed: 14990643]
7. Torres MA, Jhingran A, Thames HD Jr, et al. Comparison of treatment tolerance and outcomes in patients with cervical cancer treated with concurrent chemoradiotherapy in a prospective randomized trial or with standard treatment. Int J Radiat Oncol Biol Phys. 2008; 70(1):118–125. [PubMed: 17869451]
8. Chemoradiotherapy for Cervical Cancer Meta-analysis Collaboration. Reducing uncertainties about the effects of chemoradiotherapy for cervical cancer: Individual patient data meta-analysis. J Clin Oncol. 2008; 26:5802–5812. [PubMed: 19001332]
9. WHO handbook for reporting results of cancer treatment, Publication Number 48. Geneva: World Health Organization; 1979. Available at: http://whqlibdoc.who.int.publications/9241700483.pdf
10. James K, Eisenhauer E, Christian M, et al. Measuring response in solid tumors: Unidimensional versus bidimensional measurement. J Natl Cancer Inst. 1999; 91:523–528. [PubMed: 10088622]
11. Kastritis E, Bamias A, Efstathiou E, et al. The outcome of advanced or recurrent non-squamous carcinoma of the uterine cervix after platinum-based combination chemotherapy. Gynecol Oncol. 2005; 99:376–382. [PubMed: 16051322]
12. Brizel DM, Rosner GL, Prosnitz LR, et al. Patterns and variability of tumor oxygenation in human soft tissue sarcomas, cervical carcinomas and lymph node metastases. Int J Radiat Oncol Biol Phys. 1995; 32:1121–1125. [PubMed: 7607933]
13. Koukourakis MI, Giatromanolaki A, Sivridis E, et al. Cancer vascularization: Implications in radiotherapy? Int J Rad Oncol Biol Phys. 2000; 48:545–553.
14. Pugachev A, Ruan S, Carlin S. Dependence of FDG uptake on tumor microenvironment. Int J Radiat Oncol Biol Phys. 2005; 62:545–553. [PubMed: 15890599]
15. Bachtiary B, Boutros PC, Pintilie M. Gene expression profiling in cervical cancer: An exploration of intratumor heterogeneity. Clin Cancer Res. 2006; 12:5632–5640. [PubMed: 17020965]
16. Britten RA, Evans AJ, Allalunis-Turner MJ, et al. Intratumoral heterogeneity as a confounding factor in clonogenic assays for tumour radioresponsiveness. Radiother Oncol. 1996; 39:145–153. [PubMed: 8735482]
17. Galmarini FC, Galmarini CM, Sarchi MI, et al. Heterogeneous distribution of tumor blood supply affects the response to chemotherapy in patients with head and neck cancer. Microcirculation. 2000; 7:405–410. [PubMed: 11142337]
18. Höckel M, Schlenger K, Mitze M, et al. Hypoxia and radiation response in human tumors. Semin Radiat Oncol. 1996; 6:3–9. [PubMed: 10717157]
19. Dunst J, Kuhnt T, Strauss HG, et al. Anemia in cervical cancers: impact on survival, patterns of relapse, and association with hypoxia and angiogenesis. Int J Radiat Oncol Biol Phys. 2003; 56:778–787. [PubMed: 12788185]
20. Vaupel, P. Oxygenation of solid tumors. In: Teicher, BA., editor. Drug resistance in oncology. New York: Marcel Dekker; 1993. p. 53-85.
21. Latargau E, Randranarivelo HLM. Oxygen tension measurements in human tumors: The Institute Gustave-Roussy experience. Radiat Oncol Invest. 1994; 1:285–291.

22. Urtasun RC, Chapman JD, JAR, et al. Binding of H-3-misonidazole to solid human tumors as a measure of tumor hypoxia. Int J Radiat Oncol Biol Phys. 1986; 12:1263–1267. [PubMed: 3017905]
23. Brash RC, Li KC, Husband JE, et al. In vivo monitoring of tumor angiogenesis with MR imaging. Acad Radiol. 2000; 7:812–823. [PubMed: 11048879]
24. Mayr NA, Hawighorst H, Yuh WTC, et al. MR microcirculation in cervical cancer: Correlations with histomorphological tumor markers and clinical outcome. J Magn Reson Imaging. 1999; 10:267–276. [PubMed: 10508286]
25. Brix G, Rempp K, Guckel F. Quantitative assessment of tissue microcirculation by dynamic contrast-enhanced MR imaging. Adv MRI Contrast. 1994; 2:68–77.
26. Neeman M, Dafni H. Structural, functional, and molecular MR imaging of the microvasculature. Ann Rev Biomed Eng. 2003; 5:29–56. [PubMed: 14527310]
27. Link KH, Leder G, Pillasch J. *In vitro* concentration response studies and *in vitro* Phase II tests as the experimental basis for regional chemotherapeutic protocols. Semin Surg Oncol. 1998; 14:189–201. [PubMed: 9548601]
28. Minchinton AI, Tannock IF. Drug penetration in solid tumours. Nat Rev Cancer. 2006; 6:583–592. [PubMed: 16862189]
29. Ellingsen C, Natvig I, Gaustad JV, et al. Human cervical carcinoma xenograft models for studies of the physiological microenvironment of tumors. J Cancer Res Clin Oncol. 2009; 135:1177–1184. [PubMed: 19214568]
30. Yuh WTC. An exciting and challenging role for the advanced contrast MR imaging. J Magn Reson Imaging. 1999; 10:221–222. [PubMed: 10508280]
31. Yuh WTC, Mayr NA, Jarjoura D, et al. Predicting control of primary tumor and survival by DCE MRI during early therapy in cervical cancer. Invest Radiol. 2009; 44:343–350. [PubMed: 19661844]
32. Mayr NA, Yuh WTC, Magnotta VA, et al. Tumor perfusion studies using fast magnetic resonance imaging technique in advanced cervical cancer—A new noninvasive predictive assay. Int J Radiat Oncol Biol Phys. 1996; 36:623–633. [PubMed: 8948347]
33. Gong QY, Brunt JN, Romaniuk CS, et al. Contrast enhanced dynamic MRI of cervical carcinoma during radiotherapy: Early prediction of tumour regression rate. Br J Radiol. 1999; 72:1177–1184. [PubMed: 10703475]
34. Loncaster JA, Carrington BM, Sykes JR, et al. Prediction of radiotherapy outcome using dynamic contrast enhanced MRI of carcinoma of the cervix. Int J Rad Oncol Biol Phys. 2002; 54:759–767.
35. Yamashita Y, Baba T, Baba Y, et al. Dynamic contrast-enhanced MR imaging of uterine cervical cancer: Pharmacokinetic analysis with histopathologic correlation and its importance in predicting the outcome of radiation therapy. Radiology. 2000; 216:803–809. [PubMed: 10966715]
36. Mayr NA, Yuh WTC, Arnholt JC, et al. Pixel analysis of MR perfusion imaging in predicting radiation therapy outcome in cervical cancer. J Magn Reson Imaging. 2000; 12:1027–1033. [PubMed: 11105046]
37. Zahra MA, Tan LT, Priest AN, et al. Semiquantitative and quantitative dynamic contrast-enhanced magnetic resonance imaging measurements predict radiation response in cervix cancer. Int J Radiat Oncol Biol Phys. 2009; 74:766–773. [PubMed: 19019563]
38. Mayr NA, Yuh WTC, Jajoura D, et al. Ultra-early predictive assay for treatment failure using functional magnetic resonance imaging and clinical prognostic parameters in cervical cancer. Cancer. 2010; 116:903–912. [PubMed: 20052727]
39. Weidner N. Tumoral vascularity as a prognostic factor in cancer patients: The evidence continues to grow. J Pathol. 1998; 184:119–122. [PubMed: 9602700]
40. Green JA, Kirwan JM, Tierney JF, et al. Survival and recurrence after concomitant chemotherapy and radiotherapy for cancer of the uterine cervix: A systematic review and meta-analysis. Lancet. 2001; 358:781–786. [PubMed: 11564482]

Summary

The functional risk volume (FRV) is the absolute volume within the heterogeneous tumor that is characterized by low dynamic contrast enhancement, indicative of poor perfusion and hypoxia. This outcome study in cervical cancer patients shows that FRV correlates with local tumor control, disease specific and overall survival. FRV appears to be a better predictor of therapy outcome than the anatomical tumor volume.

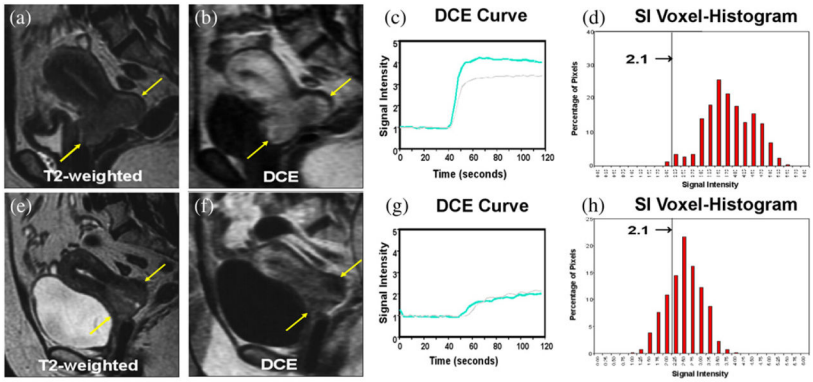

Fig. 1.

Heterogeneity of dynamic contrast-enhanced (DCE) and low perfusion. (a–d) Patient with a large Stage IIB cervical cancer (a, arrows) clinically expected to have poor outcome. At 2 weeks of therapy, this tumor shows intense enhancement (b, arrows), high perfusion on the DCE curve (c; gray: pretreatment, blue: early treatment). (d) Signal intensity (SI) voxel-histogram shows that most tumor voxels have high tumor perfusion (SI ≥2.1). This patient has been disease-free for more than 10 years. (e–h) Another Stage IIB patient with a smaller tumor (e, arrows) clinically expected to have excellent outcome. At 2 weeks, this tumor shows poor enhancement (f, arrows) and low perfusion on the DCE curve (g). (h) SI voxel-histogram shows that a much larger proportion of tumor voxels are classified as at-risk voxels (SI <2.1), compared with panel d. This patient had tumor recurrence 3 months after therapy and died 6 months later. Figure adapted with permission from Mayr NA *et al. J Magn Reson Imaging* 2000;12:1027–1033.

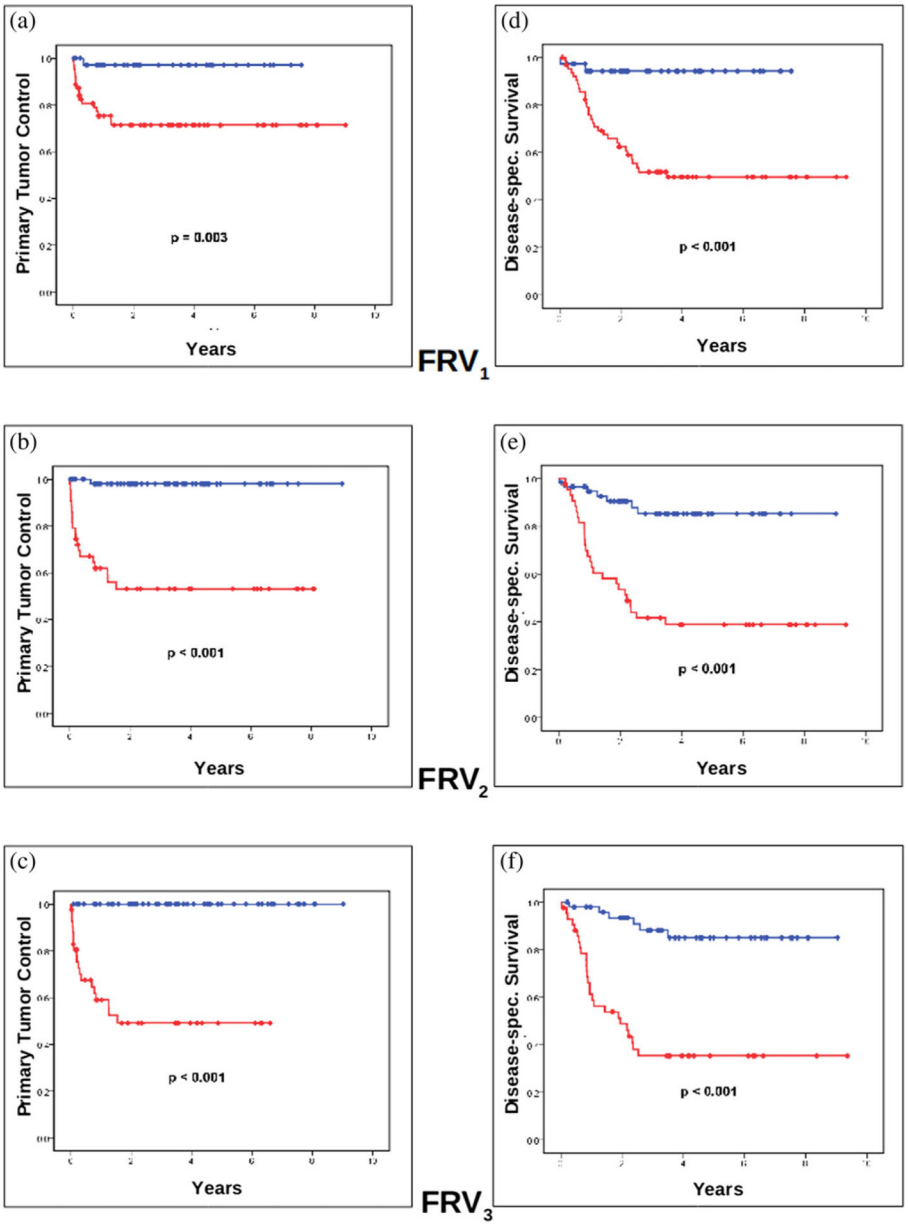

Fig. 2.

Kaplan-Meier analysis of primary tumor control and disease-specific survival. Kaplan-Meier estimates differentiate primary tumor control rate vs. tumor recurrence for (a) FRV_1, (b) FRV_2, and (c) FRV_3. Kaplan-Meier estimates for disease-specific survival rate vs. death from disease for (d) FRV_1, (e) FRV_2, and (f) FRV_3. The blue graphs indicate groups with FRV above cutpoint, the red graphs groups below the FRV cutpoint. More detailed statistical analysis is summarized in Tables 3 and 4. FRV = functional risk volume; spec. = specific.

Table 1

Patient characteristics

Criteria	Patient number	Percentage
Age		
Mean (years)	52	–
Range	25–89	
FIGO stage		
I–II	60	59
III–IV	42	41
Tumor size		
<6 cm	33	32
≥6 cm	69	68
Lymph nodes		
Uninvolved	71	70
Involved	31	30
Local control		
Local control	81	–
Central failure*	6	
Pelvic failure†	15	
Death of disease		
Alive	62	–
Dead of disease	40	

Abbreviation: FIGO = International Federation of Gynecology and Obstetrics.

*Failure in primary tumor/uterus without lateral pelvic or nodal failure.

†Recurrence in pelvic nodes and or parametria with or without central failure.

Table 2

Mean, range, and SD of ATVs and FRVs at the three imaging time points

	ATV_1	ATV_2	ATV_3	FRV_1	FRV_2	FRV_3
Mean	74.421	42.097	17.187	42.513	19.633	8.941
Range	4.3–341.7	1.9–307.3	0–191.8	1.03–237.8	0.57–123.1	0–62.2
SD	62.062	44.798	24.683	45.314	23.359	12.149

Abbreviations: ATV = anatomic tumor volume; FRV = functional risk volume.

Table 3

Correlation of FRV with primary tumor control

	FRV_1	FRV_2	FRV_3
Below FRV cutpoint vs. Above FRV cutpoint	97.3% vs. 73.0%	98.3% vs. 55.8%	100.0% vs. 54.8%
p (Kaplan-Maier)	0.003	7.3×10^{-8}	2.0×10^{-8}
p (Mann-Whitney)	0.002	1.0×10^{-7}	1.5×10^{-8}

Abbreviation: FRV = functional risk volume.

The FRV cutpoints, determined by receiver operator characteristic analysis to differentiate between favorable and poor outcomes, are 20 cm^3 (FRV_1), 13 cm^3 (FRV_2), and 5 cm^3 (FRV_3), derived from DCE-MR obtained before, at 2–2.5 weeks, or 4–5 weeks into treatment, respectively. Intratreatment FRV_2 and FRV_3, which are obtained after exposure to cytotoxic treatment, show larger deferences than FRV_1 in the predicted tumor treatment outcome.

Table 4

Correlation of FRV with disease-specific survival

	FRV_1	FRV_2	FRV_3
Below FRV cutpoint vs. Above FRV cutpoint	94.6% vs. 53.1%	87.9% vs. 40.9%	88.0% vs. 39.5%
p (Kaplan-Maier)	1.9×10^{-4}	2.1×10^{-6}	2.5×10^{-7}
p (Mann-Whitney)	1.8×10^{-4}	7.3×10^{-7}	4.6×10^{-6}

Abbreviation: FRV = functional risk volume.

FRV cutpoints and timing as in Table 2.

Table 5

Comparison of ATVs and FRVs as independent predictors for primary tumor control and disease-specific survival

	ATV_1	ATV_2	ATV_3	FRV_1	FRV_2	FRV_3
Local control						
p	0.567	0.175	0.077	0.065	0.020	0.004
HR	1.6	3.2	3.6	7.9	5.4	7.4
CI	0.32–8.02	0.59–17.38	0.87–14.69	0.88–68.96	1.30–22.61	1.92–28.74
Disease-specific survival						
p	0.195	0.173	0.316	0.053	0.020	<0.001
HR	1.9	2.0	0.6	4.5	3.3	7.9
CI	0.72–5.02	0.73–5.79	0.17–1.52	0.98–20.81	1.21–8.91	2.97–20.87

Abbreviations: ATV = anatomic tumor volume; CI = 95% confidence interval; FRV = functional risk volume; HR = hazard ratio.

Multivariate analysis incorporating ATV, FRV, stage and lymph node status shows that FRV_2 and FRV_3 are superior to ATVs as independent predictors of local control and disease-specific survival.

Int J Radiat Oncol Biol Phys. Author manuscript; available in PMC 2015 March 25.